

# Fluorinated Polymerizable Phosphonium Salts from PH<sub>3</sub>: Surface Properties of Photopolymerized Films

Ryan Guterman,<sup>1</sup> Bradley M. Berven,<sup>1</sup> T. Chris Corkery,<sup>1</sup> Heng-Yong Nie,<sup>2</sup> Mike Idacavage,<sup>3</sup> Elizabeth R. Gillies,<sup>1,4</sup> Paul J. Ragogna<sup>1</sup>

<sup>1</sup>Department of Chemistry and The Centre for Advanced Materials and Biomaterials Research (CAMBR), Western University, 1151 Richmond St, London, Ontario, Canada N6A 5B7

<sup>2</sup>Surface-Science Western (SSW), Western University, 999 Collip Circle, London, Ontario, Canada N6G 0J3

<sup>3</sup>Esstech, Inc., 48 Powhattan Ave., Essington, Pennsylvania 19029, USA

<sup>4</sup>Department of Chemical and Biochemical Engineering, Western University 1151 Richmond St, London, Ontario, Canada N6A 5B7

Correspondence to: P. J. Ragogna (E-mail: pragogna@uwo.ca)

Received 31 January 2013; accepted 16 March 2013; published online 19 April 2013

DOI: 10.1002/pola.26692

**ABSTRACT:** An array of highly fluorinated polymerizable phosphonium salts (HFPPS) were synthesized from PH<sub>3</sub> and utilized in UV-curable formulations. Inclusion of these salts at very low loading (0.1–1 wt %) into hexanediol diacrylate (HDDA) resulted in hydrophobic surfaces. The water repellency was achieved with short C<sub>4</sub>F<sub>9</sub> fluorocarbon appendages in the monomer as opposed to the bioaccumulative C<sub>8</sub>F<sub>17</sub> appended polymers. The physical properties of these new monomers were also characterized. The molecular architecture of the monomers had a pronounced effect on both their physical properties along with the degree of hydrophobicity imparted in the polymer. Salts utilizing the bis(trifluoromethylsulfonyl)imide anion displayed

excellent compatibility with HDDA, while the chloride salts were insoluble. Time-of-flight secondary ion mass spectrometry (TOF-SIMS) confirmed the presence of the HFPPS at the surface of the polymer coating. For the first time this demonstrates how these salts may be used to functionalize the surface of a UV-cured film with ionic species. © 2013 Wiley Periodicals, Inc. *J. Polym. Sci., Part A: Polym. Chem.* **2013**, *51*, 2782–2792

**KEYWORDS:** curing of polymers; fluorocarbon; fluoropolymers; ionic liquid; phosphonium salt; photopolymerization; poly(ionic liquid); polyelectrolytes; surfaces; UV-curing

**INTRODUCTION** The increase in popularity of photopolymerization over the past several decades has given rise to new functional materials in various fields of polymer science, from applications in biomaterials to the construction of three-dimensional microstructures.<sup>1,2</sup> The breadth of new monomers, oligomers, and additives used in industry and academia is a consequence of this expansion, and the possible applications for photopolymerization are simply limited by the feedstocks available. There exists an expanding niche within this area for more exotic molecules that can only be filled by modern research in synthetic chemistry.

Phosphonium salts are a class of molecules with highly tunable properties that have been used in polymer science.<sup>3–7</sup> By manipulating the molecular architecture around the phosphonium centre, both the physical and chemical properties can be varied. Our research focus in this context includes chemical functionality of the phosphonium cation for

hydrophobic performance, and synthetic tunability of the counter anion to alter material hardness.<sup>8,9</sup> Recently, there has been a growing interest in using phosphonium salts in polymerizable systems. This includes the work of Gin and Long who have demonstrated the use of the phosphonium scaffold for various applications.<sup>10–13</sup> Much of the work of Long and coworkers in this context is based on thermal polymerization methodologies with the synthesis of various phosphonium homopolymers and copolymers. We are interested in applying similar monomers to polymer networks synthesized using photoinitiated processes.<sup>9</sup> Despite the rich chemistry of phosphorus and ease with which it can be manipulated, the utility of the polymerizable phosphonium salt has not been widely exploited within photopolymer applications.<sup>10</sup>

Ionic materials in general have been used in UV-cured systems and possess some noteworthy applications. For example, inorganic salts infused into photopolymers have been

Additional Supporting Information may be found in the online version of this article.

© 2013 Wiley Periodicals, Inc.

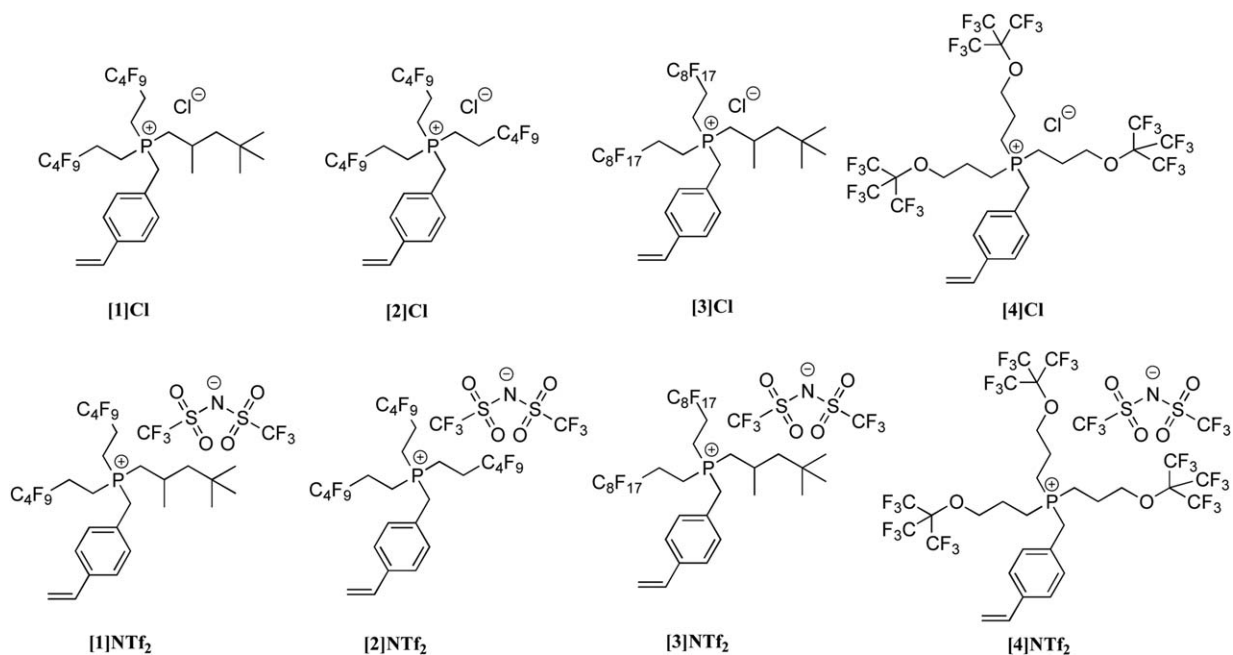


**FIGURE 1** All HFPSS synthesized in this study for applications in photopolymerizable systems.

used for the purpose of fabricating electrically conductive coatings.<sup>14</sup> Organic salts have been shown to assist in the dispersion of charged particles.<sup>15–17</sup> Despite these previous examples, there have been no reports of surface modification using phosphonium salts within the UV-curing field. Previous work from our group demonstrated that a monolayer of thiol-appended, fluorinated phosphonium salts on roughened metal surfaces exhibited excellent water repellency with water contact angles of up to 168°. These proof-of-concept experiments demonstrated that the phosphonium ion scaffold could be used to generate coatings with poor wettability when functionalized with fluorocarbon appendages.<sup>18</sup> On the downside, these films were highly delicate and any physical contact with the surface resulted in a complete loss of performance. One solution to address film resiliency was to incorporate polymerizable groups onto the phosphorus centre in place of a thiol (Fig. 1). Such functionality would allow for the incorporation of phosphonium salts into photopolymerizable systems to afford durable films while ideally maintaining hydrophobic character. The tunable nature of phosphonium chemistry also allows for a wide array of different cations, each with uniquely different physical and chemical properties. Such control highlights this class of molecule as a potential candidate for wide applications in photopolymerization technologies where such regulation is critical. As polymerizable fluorocarbons are already being used in photopolymer systems, there may be room for improvement through varying molecular architecture of the active species.<sup>19–21</sup> In this context, we demonstrate the incredible variety and tailorability of phosphonium salts for the surface modification of photopolymerizable systems. Depending on the substitution around the phosphonium core and anion size/composition, the surface wettability can be drastically altered.

## EXPERIMENTAL

All compounds were synthesized under a N<sub>2</sub> atmosphere or prepared in a nitrogen-filled MBraun Labmaster 130 glove box unless otherwise noted. Cytop 183 (2,4,4-trimethylpentyl)phosphine, 2,2,4-trimethylpentyl-bis(1H,1H,2H,2H-perfluorohexyl)phosphine, HDMA (2-hydroxy-2-methyl-1-phenyl-propanone), HDDA (hexanediol diacrylate), and EB130 were donated by Cytec Corporation and used as received. Lithium bis(trifluoromethylsulfonyl)imide was purchased from Alfa Aesar and used as received. Solvents were purchased from Caledon and dried using an MBraun Solvent Purification System. The fluorinated precursors bis(1H,1H,2H,2H-perfluorooctyl)(2,4,4-trimethylpentyl)phosphine, tris(1H,1H,2H,2H-perfluorohexyl)phosphine and sodium nonafluoro-*tert*-butoxide were prepared using literature procedures, respectively.<sup>18,22,23</sup> Dried solvents were collected under vacuum in a flame dried Strauss flask and stored over 4 Å molecular sieves in the drybox. Deuterated chloroform was purchased from Caledon and stored over 4 Å molecular sieves in the drybox. 4-Vinylbenzyl chloride and acetone-*d*<sub>6</sub> were purchased from Sigma Aldrich and used as received. PH<sub>3</sub> (pressurized cylinder) was obtained from Cytec Corporation and was used as received.

**Caution!** PH<sub>3</sub> is a pyrophoric and toxic gas. It should be handled with extreme caution, including the use of PH<sub>3</sub> monitors, a stainless steel manifold, and deliberate burning of waste streams for eventual conversion into H<sub>3</sub>PO<sub>4</sub> (via P<sub>4</sub>O<sub>10</sub>). Further details are described below in the synthesis of tris(nonafluoro-*tert*-butoxypropyl)phosphine, and photos of the manifold are included in Supporting Information Figs. S-33 and S-34.

Nuclear Magnetic Resonance (NMR) spectroscopy was conducted on a Varian INOVA 400 MHz spectrometer (<sup>1</sup>H

400.09 MHz,  $^{31}\text{P}\{^1\text{H}\}$  161.82 MHz,  $^{19}\text{F}\{^1\text{H}\}$  376.15 MHz). All  $^1\text{H}$  spectra were referenced relative to incompletely deuterated solvent signals ( $\text{CDCl}_3$ ;  $^1\text{H}$   $\delta\text{H} = 7.26$  ppm and  $\text{CO}(\text{CD}_3)_2$ ;  $^1\text{H}$   $\delta\text{H} = 2.04$ ). The chemical shifts for  $^{31}\text{P}\{^1\text{H}\}$  and  $^{19}\text{F}\{^1\text{H}\}$  NMR spectroscopy were referenced using an external standard (85%  $\text{H}_3\text{PO}_4$   $\delta\text{P} = 0$ ; trifluorotoluene,  $\text{PhCF}_3$   $\delta\text{F} = -63.9$  ppm). Infrared spectra were recorded using a Bruker Tensor 27 spectrometer with an attenuated total reflectance (ATR) attachment using a ZnSe crystal (resolution  $4\text{ cm}^{-1}$ ). Sonication of the UV curable formulations was conducted in an E60H Elmasonic sonicator at frequency of 37 kHz using an effective power of 100 W. Deposition of the formulation was performed using a 25- $\mu\text{m}$  Meyer Rod purchased from Gardco on microscope slides purchased from Technologist Choice unless otherwise noted. UV curing was performed using a modified UV curing system purchased from UV Process and Supply with a mercury bulb. Water contact angles (WCA) were measured with a 5  $\mu\text{L}$  drop using a Kruss DSA100 Drop Shape Analyzer. Thermal degradation was determined using Thermal Gravimetric Analysis (TGA) on a Q600 SDT TA instrument: a sample of 5–15 mg was placed in an Alumina cup and heated at a rate of  $10\text{ }^\circ\text{C}/\text{min}$  from room temperature to  $600\text{ }^\circ\text{C}$  under nitrogen atmosphere (100 mL/min). Glass transition temperatures were determined using Differential Scanning Calorimetry (DSC) on a DSC Q20 TA instrument: a sample of approximately 10 mg was placed in an aluminum Tzero pan and underwent a heat/cool/heat profile at  $10\text{ }^\circ\text{C}/\text{min}$  under nitrogen atmosphere (50 mL/min). The transitions were determined from the final heat cycle of the heat/cool/heat profile. Melting points of all HFPPS were determined using a Gallenkamp Variable Heater in air. Mass spectrometry was recorded in both positive and negative ion modes using an electrospray ionization (ESI) Micromass LCT spectrometer. Elemental analysis (EA) was performed by the Elemental Analysis Laboratory at the Université de Montréal. Time-of-flight Secondary Ion Mass Spectrometry (TOF-SIMS) measurements were performed using an ION-TOF (GmbH) TOF-SIMS IV equipped with a Bi cluster liquid metal ion source. A 25 keV  $\text{Bi}_3^+$  cluster primary pulsed ion beam (10 kHz, pulse width 2 ns) was used to bombard the surface to generate secondary ions. The positive or negative secondary ions were extracted from the sample surface, mass separated and detected via a reflectron-type time-of-flight analyzer. Depth profiles were obtained by repeating the following cycle: sputtering an area of  $500 \times 500\text{ }\mu\text{m}^2$  on the sample surface with a 3 keV  $\text{Cs}^+$  ion beam for 0.5 s followed by, with a delay of 2 s, collecting mass spectra at  $128 \times 128$  pixels with the  $\text{Bi}_3^+$  ion beam over an area of  $245 \times 245\text{ }\mu\text{m}^2$  in the centre of the sputtered area. Surface morphology was imaged using dynamic force mode on a Park Systems XE-100 atomic force microscope (AFM). A silicon cantilever having a nominal spring constant of 40 N/m, resonant frequency of 300 kHz and a tip radius of 10 nm was used. In the dynamic force mode, the cantilever was vibrated near its resonant frequency and its reduced oscillation amplitude was used as the feedback parameter to image the surface. Images of  $256 \times 256$  pixels on an area of  $20 \times 20\text{ }\mu\text{m}^2$  were collected.

### Solubility/Miscibility Tests

Approximately 5 mg of compound was added to a test tube followed by the addition of 1.5 mL of solvent and gentle stirring. If dissolution was not observed, the mixture was further stirred and sonicated for 30 s. Material was deemed soluble if the resulting solution was free of particulate and haze, as determined by visual inspection. Material was deemed insoluble if a large majority of the powder did not dissolve. In two cases however, hazy mixtures were formed that we believed to be emulsion.

### Film Preparation

A desired amount of photoinitiator (5 wt % HDMAP), crosslinker (HDDA), and phosphonium salt were weighed and combined in screw top vials. The mixture was sonicated at  $45\text{ }^\circ\text{C}$  for 20 min until the solutions were free of particulate and haze. After cooling to room temperature, the solutions were cast on glass slides using a Meyer rod (25  $\mu\text{m}$ ), placed on a conveyor and irradiated with UV light (Irradiance—UVA:  $412\text{ mW}/\text{cm}^2$  UVB:  $423\text{ mW}/\text{cm}^2$  UVC:  $79\text{ mW}/\text{cm}^2$ . Energy Density - UVA:  $234\text{ mJ}/\text{cm}^2$  UVB:  $238\text{ mJ}/\text{cm}^2$  UVC:  $45\text{ mJ}/\text{cm}^2$ ).

### Synthesis of [1]Cl

2,2,4-trimethylpentyl-bis(1*H*,1*H*,2*H*,2*H*-perfluorohexane)phosphine (8.04 g, 12.60 mmol) and 4-vinylbenzyl chloride (3.85 g, 25.19 mmol) were dissolved in dimethylformamide (7 mL) and heated to  $120\text{ }^\circ\text{C}$  under an  $\text{N}_2$  atmosphere. The reaction was monitored by  $^{31}\text{P}\{^1\text{H}\}$  NMR spectroscopy and was complete after 3 h. The product was precipitated in hexanes as a light brown solid. Reprecipitation (5 mL dichloromethane into 200 mL hexanes, followed by stirring in isopentane) yielded an off-white powder. (4.77 g, 54%); Anal. Calcd for  $\text{C}_{29}\text{H}_{34}\text{ClF}_{18}\text{P}$ : C 44.04%, H 4.33%. Found: C 44.91%, H 4.08%.  $T_m$ :  $95.3\text{--}95.7\text{ }^\circ\text{C}$ . IR:  $\nu(\text{C—F})$   $1133\text{ cm}^{-1}$ ,  $\nu(\text{HC}=\text{CH}_2)$   $990\text{ cm}^{-1}$ .

$^1\text{H}$  NMR (acetone- $d_6$ ,  $\delta$ ) 7.60 (d, 2H,  $^3J = 10.8$  Hz, Ar- $\text{H}_{\text{ortho}}$ ), 7.38 (d, 2H,  $^3J = 8.0$  Hz, Ar- $\text{H}_{\text{meta}}$ ), 6.64 (dd, 1H,  $^3J = 17.4$  Hz (trans),  $^3J = 10.8$  Hz (cis),  $\text{CH}=\text{CH}_2$ ), 5.72 (d, 1H,  $^3J = 17.4$  Hz,  $\text{CH}=\text{CH}_2$ -trans), 5.15 (d, 1H,  $^3J = 11.4$  Hz,  $\text{CH}=\text{CH}_2$ -cis), 4.85 (d, 2H,  $^3J = 16.0$  Hz, Ar- $\text{CH}_2$ ), 3.18–2.91 (m, 4H,  $\text{PCH}_2\text{CH}_2$ ), 2.82–2.65 (m, 6H,  $\text{PCH}_2$ ), 2.38–2.26 (m, 1H,  $\text{PCH}_2\text{CH}$ ), 1.51–1.28 (m, 2H,  $\text{CHCH}_2\text{C}(\text{CH}_3)_3$ ), 1.21 (d, 2H,  $^3J = 6.4$  Hz,  $\text{CHCH}_3$ ), 0.89 (s, 9H,  $\text{C}(\text{CH}_3)_3$ ).  $^{19}\text{F}\{^1\text{H}\}$  NMR (acetone- $d_6$ ,  $\delta$ )  $-80.9$  to  $-81.2$  (m, 6F),  $-114.75$  (bs, 2F),  $-123.68$  (bs, 2F),  $-125.90$  (bs, 2F);  $^{31}\text{P}\{^1\text{H}\}$  NMR (acetone- $d_6$ ,  $\delta$ ) 35.7 (s). MS (ESI+, %): 755.1 ([cation] $^+$ , 100), 1545.3 ([cation] $_2$  + anion] $^+$ , 30). MS (ESI-, %): 825.1 ([M+Cl] $^-$ , 10), 689.1 ([M-C $_6\text{H}_4\text{CH}=\text{CH}_2$ ] $^-$ , 10).

### Synthesis of [1]NTf<sub>2</sub>

Compound [1]Cl (1.09 g, 1.37 mmol) and lithium bis(trifluoromethylsulfonyl)imide (0.800 g, 2.74 mmol) were dissolved in dichloromethane (12 mL) and allowed to stir under a  $\text{N}_2$  atmosphere. Once there was no further visible accumulation of precipitate (40 h), the reaction mixture was partitioned between dichloromethane (100 mL) and water (100 mL). The organic layer washed with water ( $2 \times 100$

mL), dried with MgSO<sub>4</sub>, and then the solvent was removed. The resulting pale yellow oil was triturated with diethyl ether/hexanes (10/90, 50 mL) to afford a white powder that was filtered and dried *in vacuo*. (1.24 g, 87%); Anal. Calcd for C<sub>31</sub>H<sub>34</sub>F<sub>24</sub>NO<sub>4</sub>PS<sub>2</sub>: C 35.95%, H 3.31%, N 1.35%. Found: C 36.19%, H 3.31%, N 1.27%. *T*<sub>m</sub>: 88.1–88.8 °C. IR: ν(C–F anion) 1347 cm<sup>-1</sup>, ν(C–F cation) 1135 cm<sup>-1</sup>, ν(SO<sub>2</sub>) 1057 cm<sup>-1</sup>, ν(HC=CH<sub>2</sub>) 988 cm<sup>-1</sup>.

<sup>1</sup>H NMR (acetone-*d*<sub>6</sub>, δ) 7.57 (d, 2H, <sup>3</sup>*J* = 7.6 Hz, Ar-H<sub>ortho</sub>), 7.48 (d, 2H, <sup>3</sup>*J* = 7.6 Hz, Ar-H<sub>meta</sub>), 6.76 (dd, 1H, <sup>3</sup>*J* = 17.4 Hz (trans), <sup>3</sup>*J* = 10.8 Hz (cis), CH=CH<sub>2</sub>), 5.84 (d, 1H, <sup>3</sup>*J* = 18.0 Hz, CH=CH<sub>2</sub>-trans), 5.30 (d, 1H, <sup>3</sup>*J* = 10.8 Hz, CH=CH<sub>2</sub>-cis), 4.34 (d, 2H, <sup>3</sup>*J* = 16.0 Hz, Ar-CH<sub>2</sub>), 3.08–3.01 (m, 4H, PCH<sub>2</sub>CH<sub>2</sub>), 2.86–2.74 (m, 6H, PCH<sub>2</sub>), 2.43–2.31 (m, 1H, PCH<sub>2</sub>CH), 1.51–1.40 (m, 2H, CHCH<sub>2</sub>C(CH<sub>3</sub>)<sub>3</sub>), 1.27 (d, 3H, <sup>3</sup>*J* = 6.4 Hz, CHCH<sub>3</sub>), 0.92 (s, 9H, C(CH<sub>3</sub>)<sub>3</sub>); <sup>19</sup>F{<sup>1</sup>H} NMR (acetone-*d*<sub>6</sub>, δ) –80.0 (s, 6F), –81.9 to –82.0 (m, 6F), –115.6 to –115.7 (m, 4F), –124.5 (bs, 4F), –126.6 to –126.7 (m, 4F). <sup>31</sup>P{<sup>1</sup>H} NMR (acetone-*d*<sub>6</sub>, δ) 34.5 (s). MS (ESI+, %) : 755.1 ([cation]<sup>+</sup>, 100), 1790.3 ([([cation]<sub>2</sub> + anion)]<sup>+</sup>, 10). MS (ESI-, %) : 1314.9 ([cation + (anion)<sub>2</sub>]<sup>-</sup>, 50), 281.2 ([NTf<sub>2</sub>]<sup>-</sup>, 100)

### Synthesis of [2]Cl

Tris(1*H*,1*H*,2*H*,2*H*-perfluorohexyl)phosphine (5.15 g, 6.67 mmol) and 4-vinylbenzyl chloride (2.12 g, 13.34 mmol) were dissolved in dimethylformamide (8 mL) and heated to 120 °C while stirring under a N<sub>2</sub> atmosphere. The reaction was monitored by <sup>31</sup>P{<sup>1</sup>H} NMR spectroscopy and was complete after 3 h. The reaction mixture was precipitated into benzene, filtered, redissolved in acetone and freeze dried *in vacuo*, yielding off-white crystals (3.37 g, 55%); Anal. Calcd for C<sub>27</sub>H<sub>21</sub>ClF<sub>27</sub>P: C 35.06%, H 2.29%. Found: C 35.07%, H 2.28%. *T*<sub>m</sub>: 79.5–81.4 °C. IR: ν(C–F) 1133 cm<sup>-1</sup>, ν(HC=CH<sub>2</sub>) 990 cm<sup>-1</sup>.

<sup>1</sup>H NMR (acetone-*d*<sub>6</sub>, δ) 7.71 (d, 2H, <sup>3</sup>*J* = 9.6 Hz Ar-H<sub>ortho</sub>), 7.45 (d, 2H, <sup>3</sup>*J* = 8.4 Hz, Ar-H<sub>meta</sub>), 6.73 (dd, 1H, <sup>3</sup>*J* = 17.6 Hz (trans), <sup>3</sup>*J* = 10.8 Hz (cis), CH=CH<sub>2</sub>), 5.80 (d, 1H, <sup>3</sup>*J* = 17.6 Hz, CH=CH<sub>2</sub>-trans), 5.26 (d, 1H, <sup>3</sup>*J* = 11.2 Hz, CH=CH<sub>2</sub>-cis), 5.15 (d, 2H, <sup>3</sup>*J* = 16.8 Hz, Ar-CH<sub>2</sub>), 3.47–3.35 (m, 6H, PCH<sub>2</sub>CH<sub>2</sub>), 3.02–2.88 (m, 6H, PCH<sub>2</sub>). <sup>19</sup>F{<sup>1</sup>H} NMR (acetone-*d*<sub>6</sub>, δ) –82.1 (s, 9F), –115.5 to –115.6 (m, 6F), –124.5 (bs, 6F), –126.7 to –126.8 (m, 6F). <sup>31</sup>P{<sup>1</sup>H} NMR (acetone-*d*<sub>6</sub>, δ) 38.0 (s). MS (ESI+, %) : 889.0 ([cation]<sup>+</sup>, 100). MS (ESI-, %) : 959.0 ([M + Cl]<sup>-</sup>, 40), 822.9 ([M - C<sub>6</sub>H<sub>4</sub>CH=CH<sub>2</sub>]<sup>-</sup>, 100).

### Synthesis of [2]NTf<sub>2</sub>

Compound [2]Cl (1.60 g, 1.73 mmol) and lithium bis(trifluoromethylsulfonyl)imide (1.14 g, 3.97 mmol) were dissolved in chloroform/benzotrifluoride (1:1, 20 mL) and allowed to stir under a N<sub>2</sub> atmosphere (48 h). The reaction mixture was partitioned between benzotrifluoride (50 mL) and water (50 mL), washed with water (2 × 50 mL), dried (MgSO<sub>4</sub>), and the volatiles removed. The oily product was triturated in dichloromethane to afford a white solid that was filtered, rinsed with dichloromethane (2 × 10 mL) and dried *in vacuo*. (1.25 g, 63%); Anal. Calcd for C<sub>29</sub>H<sub>21</sub>F<sub>33</sub>NO<sub>4</sub>PS<sub>2</sub>: C 29.78%, H 1.81%, N 1.20%. Found: C

29.93%, H 1.52%, N 1.19%. *T*<sub>m</sub>: 55.3–56.2 °C. IR: ν(C–F anion) 1344 cm<sup>-1</sup>, ν(C–F) 1133 cm<sup>-1</sup>, ν(SO<sub>2</sub>) 1061 cm<sup>-1</sup>, ν(HC=CH<sub>2</sub>) 990 cm<sup>-1</sup>.

<sup>1</sup>H NMR (acetone-*d*<sub>6</sub>, δ) 7.78 (d, 2H, <sup>3</sup>*J* = 8.4 Hz, Ar-H<sub>ortho</sub>), 7.50 (d, 2H, <sup>3</sup>*J* = 8.4 Hz, Ar-H<sub>meta</sub>), 6.77 (dd, 1H, <sup>3</sup>*J* = 18.0 Hz (trans), <sup>3</sup>*J* = 11.2 Hz (cis), CH=CH<sub>2</sub>), 5.87 (d, 1H, <sup>3</sup>*J* = 18.0 Hz, CH=CH<sub>2</sub>-trans), 5.31 (d, 1H, <sup>3</sup>*J* = 10.8 Hz, CH=CH<sub>2</sub>-cis), 4.45 (d, 2H, <sup>3</sup>*J* = 14.8 Hz, Ar-CH<sub>2</sub>), 3.28–3.17 (m, 6H, PCH<sub>2</sub>CH<sub>2</sub>), 2.98–2.81 (m, 6H, PCH<sub>2</sub>). <sup>19</sup>F{<sup>1</sup>H} NMR (acetone-*d*<sub>6</sub>, δ) –80.1 (s, 6F), –82.0 to –82.1 (m, 9F), –115.5 to –115.6 (m, 6F), –124.5 (s, 6F), –126.7 to –126.8 (m, 6F). <sup>31</sup>P{<sup>1</sup>H} NMR (acetone-*d*<sub>6</sub>, δ) 37.2 (s). MS (ESI+, %) : 888.9 ([cation]<sup>+</sup>, 100). MS (ESI-, %) : 1448.7 ([cation + (anion)<sub>2</sub>]<sup>-</sup>, 80), 1169.5 ([M]<sup>-</sup>, 70), 280.1 ([NTf<sub>2</sub>]<sup>-</sup>, 100).

### Synthesis of [3]Cl

A 250 mL pressure tube was charged with bis(1*H*,1*H*,2*H*,2*H*-perfluorooctyl)(2,4,4-trimethylpentyl)phosphine (5.0 g, 4.98 mmol) and two molar equivalents of 4-vinylbenzyl chloride (1.52 g, 9.96 mmol) in 100 mL of a 2:1 mixture of deoxygenated DMF and trifluorotoluene. The mixture was heated at 125 °C for 6 h. Volatiles were removed at 60 °C *in vacuo*. The viscous yellow oil was redissolved in a minimal amount of acetone (10 mL) and precipitated in stirring hexanes (100 mL). This process was repeated three additional times. The oil was heated *in vacuo* at 60 °C until a yellow solid was obtained. (4.24 g, 65%); Anal. Calcd for C<sub>37</sub>H<sub>34</sub>ClF<sub>34</sub>P: C 37.31%, H 2.88%. Found: C 37.38%, H 3.18%. *T*<sub>m</sub>: 72.5–73.5 °C; *T*<sub>g</sub>: 35 °C. IR: ν(C–F) 1145 cm<sup>-1</sup>, ν(HC=CH<sub>2</sub>) 952 cm<sup>-1</sup>.

<sup>1</sup>H NMR (acetone-*d*<sub>6</sub>, δ): δ 7.74 (d, 2H, <sup>3</sup>*J* = 8 Hz, Ar-H<sub>ortho</sub>), 7.49 (d, 2H, <sup>3</sup>*J* = 8 Hz, Ar-H<sub>meta</sub>), 6.75 (dd, 4H, <sup>3</sup>*J* = 12 Hz (trans), <sup>3</sup>*J* = 8 Hz (cis), CH=CH<sub>2</sub>), 5.84 (d, 1H, <sup>3</sup>*J* = 20 Hz, CH=CH<sub>2</sub>-trans), 5.27 (d, 1H, <sup>3</sup>*J* = 12 Hz, CH=CH<sub>2</sub>-cis), 5.00 (d, 2H, <sup>3</sup>*J* = 16 Hz, Ar-CH<sub>2</sub>), 2.54–3.40 (m, 10H, PCH<sub>2</sub> and PCH<sub>2</sub>CH<sub>2</sub>), 2.26–2.4 (m, 1H, PCH<sub>2</sub>CH), 1.51 (m, 1H, (CHCHHC(CH<sub>3</sub>)<sub>3</sub>), 1.30–1.45 (m, 1H, (CHCHHC(CH<sub>3</sub>)<sub>3</sub>)), 1.25 (d, 3H, <sup>3</sup>*J* = 8 Hz, CHCH<sub>3</sub>), 0.9 (s, 9H, C(CH<sub>3</sub>)<sub>3</sub>). <sup>19</sup>F NMR (acetone-*d*<sub>6</sub>, δ) –126.07 (s, 4F), –122.67 (m, 8F), –121.50 (m, 12F), –114.52 (s, 4F), –81.01 (t, <sup>3</sup>*J* = 8 Hz, 4F). <sup>31</sup>P{<sup>1</sup>H} NMR (acetone-*d*<sub>6</sub>, δ) 34.8 (s). MS (ES+, %) ([cation]<sup>+</sup>, 100).

### Synthesis of [3]NTf<sub>2</sub>

Dry deoxygenated DCM (15 mL) was added to a 50 mL round bottom flask followed by the addition of [3]Cl (1.04 g, 0.873 mmol). After complete dissolution, two molar equivalents of lithium bis((trifluoromethyl)sulfonyl)imide (0.125 g, 0.437 mmol) were added and the mixture was stirred for 12 h. The slurry was added to a separatory funnel followed by the addition of 30 mL of DCM. The organic layer was washed with distilled water (4 × 10 mL) and then dried with a minimal amount of sodium sulfate. Volatiles were evaporated *in vacuo* resulting in an orange viscous oil. (0.63 g, 50%); Anal. Calcd for C<sub>39</sub>H<sub>34</sub>F<sub>40</sub>NO<sub>4</sub>PS<sub>2</sub>: C 32.63% H 2.39% N 0.98% S 4.47%. Found: C 32.61% H 2.35% N 0.97% S 4.5%. *T*<sub>g</sub>: –16 °C. IR: ν(C–F anion) 1348 cm<sup>-1</sup>, ν(C–F) 1134 cm<sup>-1</sup>, ν(SO<sub>2</sub>) 1060 cm<sup>-1</sup>, ν(HC=CH<sub>2</sub>) 949 cm<sup>-1</sup>.

$^1\text{H}$  NMR (acetone- $d_6$ ,  $\delta$ ): 7.59 (d, 2H,  $^3J = 8$  Hz, Ar- $\text{H}_{\text{ortho}}$ ), 7.51 (d, 2H,  $^3J = 8$  Hz, Ar- $\text{H}_{\text{meta}}$ ), 6.79 (dd, 4H,  $^3J = 12$  Hz (trans),  $^3J = 8$  Hz (cis),  $\text{CH}=\text{CH}_2$ ), 5.85 (d, 1H,  $^3J = 18$  Hz,  $\text{CH}=\text{CH}_2$ -trans), 5.30 (d, 1H,  $^3J = 20$  Hz,  $\text{CH}=\text{CH}_2$ -cis), 4.35 (d, 2H,  $^3J = 16$  Hz, Ar- $\text{CH}_2$ ), 2.70–3.20 (m, 10H,  $\text{PCH}_2$  and  $\text{PCH}_2\text{CH}_2$ ), 2.30–2.50 (m, 1H,  $\text{PCH}_2\text{CH}$ ), 1.34–1.51 (m, 2H,  $\text{CHCH}_2\text{C}(\text{CH}_3)_3$ ), 1.30 (d, 3H,  $^3J = 8$  Hz,  $\text{CHCH}_3$ ), 0.95 (s, 9H,  $\text{C}(\text{CH}_3)_3$ ).  $^{19}\text{F}$  NMR (acetone- $d_6$ ,  $\delta$ ): -79.44 (s, 6F), -81.19 (m, 6F), -114.80 (s, 4F), -121.77 (m, 12F), -122.86 (m, 8F), -126.2 (s, 4F).  $^{31}\text{P}\{\text{H}\}$  NMR (acetone- $d_6$ ,  $\delta$ ): 35.6 (s). MS (ESI+, %): 1155 ([cation] $^+$ , 100). MS (ESI-, %): 1715 ([cation + (anion) $_2^-$ , 20).

### Synthesis of Nonafluoro-tert-butyl allyl ether

A 500 mL pressure round bottom flask was charged with sodium nonafluoro-tert-butoxide (65 g, 0.25 mol), allyl bromide (18.8 g, 0.15 mol) and DMF (150 mL, SPS purified) then heated at 90 °C for 6 h. The reaction mixture was poured into a brine solution (200 mL) and the lower organic phase was removed and fractionally distilled under ambient conditions. The first two fractions were azeotropes with water (30–40 °C @ 760 mmHg, confirmed by  $^1\text{H}$  NMR) and the final fraction was the desired olefin, nonafluoro-tert-butyl allyl ether (23.4 g, 85 mmol, 56%, 45–47 °C @ 760 mmHg).

$^1\text{H}$  NMR ( $\text{CDCl}_3$ ,  $\delta$ ):  $\delta$  5.9 (m, 1H,  $\text{CH}=\text{CH}_2$ ), 5.4 (d, 1H,  $^3J_{\text{trans}} = 16$  Hz,  $\text{CH}=\text{CH}_2$ ), 5.3 (d, 1H,  $^3J_{\text{cis}} = 10$  Hz,  $\text{CH}=\text{CH}_2$ ), 4.6 (d, 2H,  $^3J = 5$  Hz,  $\text{CH}_2$ ).  $^{19}\text{F}$  NMR ( $\text{CDCl}_3$ ,  $\delta$ ): -71.5 (s, 9F);  $^{13}\text{C}\{\text{H}\}$  NMR ( $\text{CDCl}_3$ ,  $\delta$ ):  $\delta$  131.6 (s,  $\text{CH}=\text{CH}_2$ ),  $\delta$  124.9–116.2 (q,  $^1J_{\text{C-F}} = 292$  Hz,  $\text{CF}_3$ ),  $\delta$  117.1 (s,  $\text{CH}=\text{CH}_2$ ),  $\delta$  80.1 (m,  $^2J_{\text{C-F}} = 30$  Hz,  $\text{C}(\text{CF}_3)_3$ ),  $\delta$  70.6 (s,  $\text{OCH}_2$ ). MS (ES+, %): 276.1 ([M] $^+$ , 100), 69.1 ([ $\text{CF}_3$ ] $^+$ , 57).

### Synthesis of Tris(nonafluoro-tert-butoxypropyl)phosphine

A 50 mL autoclave was charged with nonafluoro-tert-butyl allyl ether (23.4 g, 85 mmol), AIBN (1.5 g, 9.2 mmol) and purged with  $\text{N}_2$ . Then  $\text{PH}_3$  was added to a pressure of 80 psi (7.9 mmol) and the sealed autoclave was heated to 70 °C for 5 h. After cooling overnight the autoclave was recharged with  $\text{PH}_3$  to 80 psi. The contents were then heated at 70 °C for a further 3 h. After cooling the pressure vessel to 10 °C the remaining  $\text{PH}_3$  was removed by careful and continuous purging with  $\text{N}_2$  and incineration of the  $\text{PH}_3$  residues in a specifically designed burn-box. The yellow reaction mixture was then fractionally distilled under vacuum to isolate the product (6.7 g, 7.8 mmol, 31%, 70–75 °C @ 0.3 mmHg).

$^1\text{H}$  NMR ( $\text{CDCl}_3$ ,  $\delta$ ):  $\delta$  4.0 (t, 6H,  $\text{OCH}_2$ ), 1.8 (m, 6H,  $\text{PCH}_2$ ), 1.4 (m, 6H,  $\text{CH}_2\text{CH}_2\text{CH}_2$ ).  $^{19}\text{F}$  NMR ( $\text{CDCl}_3$ ,  $\delta$ ): -70.7 (s, 9F).  $^{31}\text{P}\{\text{H}\}$  NMR ( $\text{CDCl}_3$ ,  $\delta$ ): -32.4 (s).  $^{13}\text{C}\{\text{H}\}$  NMR ( $\text{CDCl}_3$ ,  $\delta$ ):  $\delta$  124.7–116.0 (q,  $^1J_{\text{C-F}} = 292$  Hz,  $\text{CF}_3$ ),  $\delta$  79.3 (m,  $^2J_{\text{C-F}} = 30$  Hz,  $\text{C}(\text{CF}_3)_3$ ),  $\delta$  70.0 (d,  $^3J_{\text{C-P}} = 14$  Hz,  $\text{OCH}_2$ ),  $\delta$  25.9 (d,  $^1J_{\text{C-P}} = 14$  Hz,  $\text{PCH}_2$ ),  $\delta$  21.9 (d,  $^2J_{\text{C-P}} = 14$  Hz,  $\text{CH}_2\text{CH}_2\text{CH}_2$ ), MS (ES+, %) 877.1 ([ $\text{O}=\text{PR}_3 - \text{H}$ ] $^+$ , 100).

### Synthesis of [4]Cl

A 70 mL glass pressure tube was charged with tris(nonafluorobutoxypropyl)phosphine (2.8 g, 3.25 mmol), 4-

vinylbenzyl chloride (0.85 g, 6.1 mmol), acetonitrile (5 mL) and trifluorotoluene (5 mL) and heated at 80 °C for 7 h. The volatiles were then removed and the remaining yellow oil was washed quickly with  $\text{Et}_2\text{O}$  ( $2 \times 5$  mL) and triturated with  $\text{Et}_2\text{O}$  at -20 °C to afford a white powder. The solid was filtered in the air on a frit and washed with cold 80/20  $\text{Et}_2\text{O}$ /hexane ( $3 \times 5$  mL), then dried under high vacuum to afford [4]Cl as a microcrystalline solid. It was recrystallized from acetone/benzene at -20 °C. (2.3 g, 2.3 mmol, 70%). Anal. Calcd for  $\text{C}_{30}\text{H}_{27}\text{ClF}_{27}\text{O}_3\text{P}$ : C 35.50%, H 2.68%. Found C 35.50%, H 2.73%.  $T_m$ : 120–122 °C; IR:  $\nu(\text{C-F})$  1154  $\text{cm}^{-1}$ ,  $\nu(\text{HC}=\text{CH}_2)$  971  $\text{cm}^{-1}$ .

$^1\text{H}$  NMR (acetone- $d_6$ ,  $\delta$ ):  $\delta$  7.6 (d, 2H,  $^3J = 8$  Hz, Ar- $\text{H}_{\text{ortho}}$ ), 7.4 (d, 2H,  $^3J = 8$  Hz, Ar- $\text{H}_{\text{meta}}$ ), 6.7 (dd, 1H,  $^3J = 20$  Hz (trans),  $^3J = 12$  Hz (cis),  $\text{CH}=\text{CH}_2$ ), 5.8 (d, 1H,  $^3J = 20$  Hz,  $\text{CH}=\text{CH}_2$ -trans), 5.2 (d, 1H,  $^3J = 12$  Hz,  $\text{CH}=\text{CH}_2$ -cis), 4.6 (d, 2H,  $^3J = 18$  Hz, Ar- $\text{CH}_2$ ), 4.2 (psuedo t, 6H,  $\text{OCH}_2$ ), 2.8 (m, 6H,  $\text{PCH}_2$ ), 2.1 (m, 6H,  $\text{CH}_2\text{CH}_2\text{CH}_2$ ).  $^{19}\text{F}$  NMR (acetone- $d_6$ ,  $\delta$ ): -71.1 (s, 27F).  $^{31}\text{P}\{\text{H}\}$  NMR (acetone- $d_6$ ,  $\delta$ ): 34.1 (s). MS (ES+, %) 978.2 ([cation] $^+$ , 100).

### Synthesis of [4]NTf<sub>2</sub>

A 20 mL vial was charged with [4]Cl (0.49 g, 0.48 mmol), lithium bis((trifluoromethyl)sulfonyl)imide (0.27 g, 0.93 mmol) and acetone (8 mL). The mixture was sparged with  $\text{N}_2$  for 10 min and then stirred for 4 h. Water (20 mL) was added and the resulting mixture was stirred vigorously for 5 min. The upper aqueous phase was then decanted and the remaining oil was dissolved in ethyl acetate (10 mL), dried ( $\text{Na}_2\text{SO}_4$ ) and rotary-evaporated to dryness. The colorless oil was then dissolved in a minimum amount of  $\text{Et}_2\text{O}$  (3 mL) and the volatiles removed under high vacuum (performed twice). Further drying for 12 h *in vacuo* afforded a white crystalline solid (0.50 g, 0.4 mmol, 83%); Anal. Calcd for  $\text{C}_{32}\text{H}_{27}\text{F}_{33}\text{NO}_7\text{PS}_2$ : C 30.51% H 2.16% N 1.11% S 5.09%. Found: C 30.72% H 2.13% N 1.10% S 5.11%.  $T_g$ : 1.9 °C.  $T_m$ : 106–108 °C. IR:  $\nu(\text{C-F anion})$  1348  $\text{cm}^{-1}$ ,  $\nu(\text{C-F})$  1154  $\text{cm}^{-1}$ ,  $\nu(\text{SO}_2)$  1058  $\text{cm}^{-1}$ ,  $\nu(\text{HC}=\text{CH}_2)$  971  $\text{cm}^{-1}$ .

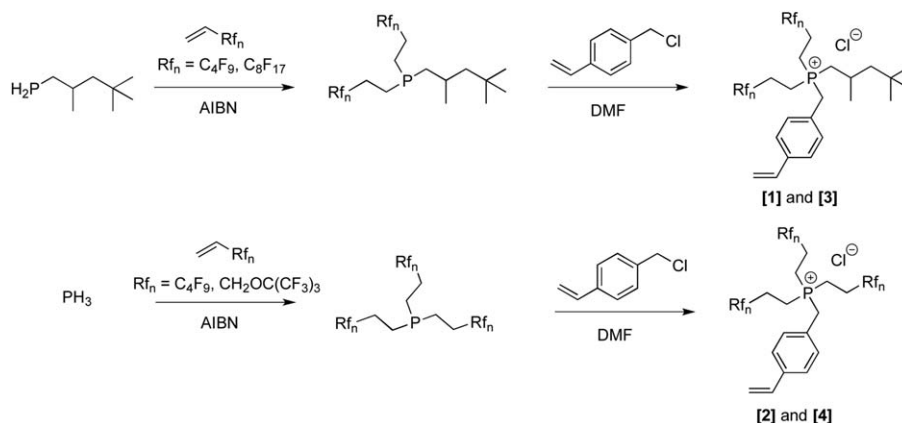
$^1\text{H}$  NMR (acetone- $d_6$ ,  $\delta$ ): 7.7 (d, 2H,  $^3J = 8$  Hz, Ar- $\text{H}_{\text{ortho}}$ ), 7.4 (d, 2H,  $^3J = 8$  Hz, Ar- $\text{H}_{\text{meta}}$ ), 6.8 (dd, 1H,  $^3J = 20$  Hz (trans),  $^3J = 12$  Hz (cis),  $\text{CH}=\text{CH}_2$ ), 5.8 (d, 1H,  $^3J = 20$  Hz,  $\text{CH}=\text{CH}_2$ -trans), 5.3 (d, 1H,  $^3J = 12$  Hz,  $\text{CH}=\text{CH}_2$ -cis), 4.3 (psuedo t, 6H,  $\text{OCH}_2$ ), 4.2 (d, 2H,  $^3J = 20$  Hz, Ar- $\text{CH}_2$ ), 2.7 (m, 6H,  $\text{PCH}_2$ ), 2.2 (m, 6H,  $\text{CH}_2\text{CH}_2\text{CH}_2$ ).  $^{19}\text{F}$  NMR (acetone- $d_6$ ,  $\delta$ ): -71.2 (s, 27F), -80.1 (s, 6F).  $^{31}\text{P}\{\text{H}\}$  NMR (acetone- $d_6$ ,  $\delta$ ): 34.8 (s). MS (ESI+, %): 1155 ([cation] $^+$ , 100). MS (ESI-, %): 1715 ([cation + (anion) $_2^-$ , 20).

## RESULTS AND DISCUSSION

### Synthesis

Phosphonium salts [1] and [3] were synthesized from the commercially available isoctyl primary phosphine while [2] and [4] required a pressurized  $\text{PH}_3$  reactor (Scheme 1).

Phosphine gas ( $\text{PH}_3$ ) is a pyrophoric substance and was manipulated with a custom built pressure-manifold. Our



**SCHEME 1** Synthetic route for the synthesis of fluororous phosphonium salts.

interest in utilizing  $\text{PH}_3$  as a starting material stems from its availability in industrial chemical manufacturing and its unique chemistry. In the presence of an olefin and a radical source (AIBN), both  $\text{PH}_3$  and primary phosphines were converted to the corresponding tertiary phosphine in one step.<sup>24</sup> A wide variety of tertiary phosphines can be synthesized, and the functional groups can be pre-selected by simply changing the olefin. This work focuses on the synthesis of fluororous phosphines and changing the architecture of the perfluoroalkyl appendage (via the olefin).<sup>22</sup> Reaction progress was monitored by  $^{31}\text{P}\{^1\text{H}\}$  NMR spectroscopy and deemed complete upon  $\sim 90\%$  conversion to the final product. Formation of the quaternary phosphonium salts proceeded through the  $\text{S}_{\text{N}}2$  reaction of a fluororous phosphine ( $\text{P}(\text{CH}_2\text{CH}_2\text{Rf}_n)_3$ ,  $\text{Rf}_n = \text{Rf}_4 = \text{C}_4\text{F}_9$  [2];  $\text{Rf}_n = \text{CH}_2\text{OC}(\text{CF}_3)_3$  [4];  $\text{R}'\text{P}(\text{CH}_2\text{CH}_2\text{Rf}_n)_2$ ,  $\text{R}' = \text{C}_8\text{H}_{17}$ ,  $\text{Rf}_n = \text{C}_4\text{H}_9$  [1];  $\text{R}' = \text{C}_8\text{H}_{17}$ ,  $\text{Rf}_n = \text{C}_8\text{F}_{17}$  [3] ( $\delta_{\text{P}} = -40$  to  $-30$  ppm) with a stoichiometric excess of 4-vinylbenzylchloride at elevated temperature (ca.,  $80^\circ\text{C}$ ), providing a broad scope of monomers. Reaction progress was monitored by  $^{31}\text{P}\{^1\text{H}\}$  NMR spectroscopy, and deemed complete when a new singlet ( $\delta_{\text{P}} = 30$ – $40$  ppm) was observed to be at a maximum. Upon work up of the reaction mixture, fluorinated phosphonium salts were isolated in 55–70% yield. Anion-exchange reactions were performed via salt-metathesis of [1–4]Cl with a stoichiometric excess of lithium bis((trifluoromethyl)sulfonyl)imide ( $\text{LiNTf}_2$ ) at room temperature for 24 h. Ion exchange reaction mixtures were extracted using distilled water to remove the inorganic salt byproduct, then volatiles were removed from the organic fraction to isolate the phosphonium bistriflamide salts in approximately 50% isolated yield.

The number and architecture of perfluoroalkyl groups were varied in order to ascertain a structure–property relationship to reveal the optimum monomer design for achieving a maximized hydrophobicity in the UV cured polymer films. It was additionally important to achieve sufficient water repellency with short perfluoroalkyl groups (i.e.,  $\text{C}_4\text{F}_9$ ), as it is well established that  $\geq \text{C}_6\text{F}_{13}$  products have been restricted by the US-EPA due to their environmental persistence.<sup>25</sup> The  $\text{C}_8\text{F}_{17}$  HFPPS monomer was included in our array to provide a

benchmark performance indicator, as it is well known that fluoropolymers containing  $\text{C}_8\text{F}_{17}$  perfluoroalkyl chains exhibit excellent hydrophobicity as a result of the organization of neighboring  $\text{C}_8\text{F}_{17}$  chains.<sup>26</sup>

Given that the constituent surface tension of the  $\text{CF}_3$  group (15 mN/m) is lower than the  $\text{CF}_2$  group (23 mN/m) we wanted to design a monomer that maximizes the number of  $\text{CF}_3$  moieties at the surface.<sup>27</sup> The solution would be to change the fluororous tail architecture from a straight-chain  $\text{C}_4\text{F}_9$  to a branched  $\text{C}_4\text{F}_9$ , thus increasing the  $\text{CF}_3$  groups to 3 per arm. Starting from perfluoro-*tert*-butanol we successfully synthesized the desired phosphonium salt [4<sup>+</sup>], which contained 9- $\text{CF}_3$  units in the cation compared to 2- $\text{CF}_3$  units for monomer [1<sup>+</sup>]/[3<sup>+</sup>] and 3- $\text{CF}_3$  units for monomer [2<sup>+</sup>] (Fig. 1).

### HFPPS Physical and Chemical Properties

In an effort to fully characterize these unconventional monomers, the solubilities of all compounds were evaluated (Fig. 2).

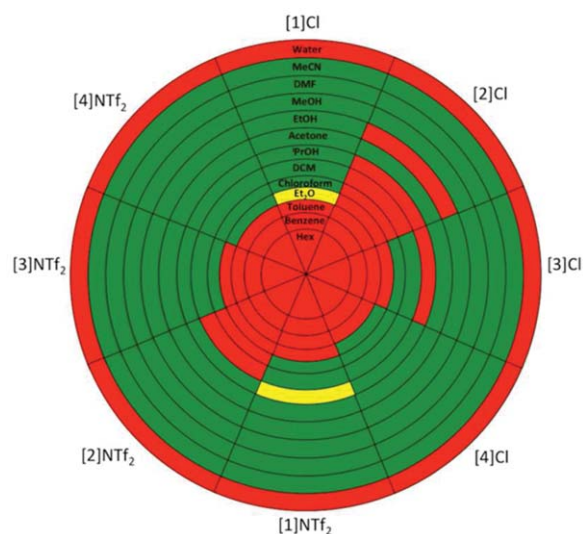


**FIGURE 2** Solubilities of all HFPPS in various polar and non-polar solvents. Green = Soluble, Red = Insoluble, Yellow = Emulsion.

**TABLE 1** Physical Properties of all HFPPS Used in this Study

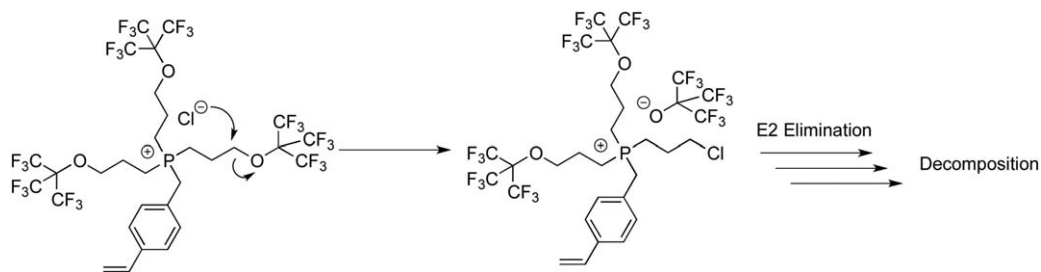
HFPPS	$T_{\text{dec}}$ (°C)	$T_g$ (°C)	m.p (°C)
[1]Cl	296	–	95–96
[2]Cl	291	–	80–81
[3]Cl	293	35	73–74
[4]Cl	197 <sup>a</sup>	–	140–142
[1]NTf <sub>2</sub>	367	–	88–89
[2]NTf <sub>2</sub>	371	–	55–56
[3]NTf <sub>2</sub>	374	–	64–69
[4]NTf <sub>2</sub>	389	1.9	106–108

<sup>a</sup> A discussion and further analysis of this observation appears below.

Although most organic molecules display predictable chemical properties (polar vs. non-polar), the solubility of phosphonium salts is highly dependent on the substitution around the phosphorus core and the counter anion. Upon the addition of fluorocarbon chains, the solubility was difficult to predict. Solvents such as H<sub>2</sub>O, hexanes, benzene and toluene proved to be poor solvents for the salts of cations 1<sup>+</sup>–4<sup>+</sup>. The fluorocarbon chains may prevent water from hydrating the cation thus preventing dissociation, while hexanes, benzene, and toluene also proved ineffective at solubilizing these charged species. Polar aprotic solvents such as DMF, acetonitrile, and acetone dissolved all compounds. Methanol was found to be an efficient protic solvent for all compounds tested while ethanol and isopropanol were successively worse in each case. Compounds [1]Cl, [1]NTf<sub>2</sub>, [3]Cl, [3]NTf<sub>2</sub>, [4]Cl, and [4]NTf<sub>2</sub> were soluble in DCM and chloroform while compounds [2]Cl and [2]NTf<sub>2</sub> were not. These results inform us of several key points relating solubility to structure. The replacement of an isoctyl chain with a fluorocarbon moiety reduces its solubility in lower polarity such as chloroform and DCM. Despite lengthening two fluorocarbon chains from C<sub>4</sub>F<sub>9</sub> to C<sub>8</sub>F<sub>17</sub>, we were still capable of solubilizing the compound. In the case of [2], the presence of three C<sub>4</sub>F<sub>9</sub> chains was sufficient to reduce its solubility. Surprisingly, both [4]Cl and [4]NTf<sub>2</sub>, displayed exceptional solubility in most solvents including diethyl ether. Despite the high fluorine loading, the branched C<sub>4</sub>F<sub>9</sub> structure along with the allyl ether linkage may impart greater solubility. The decomposition, glass transition, and melting point of these salts were measured by TGA and DSC experiments (Table 1).

The observed decomposition, glass transition, and melting points of all compounds follow a general trend characteristic of phosphonium salt structure, and previous fluorosulfonyl phosphonium salts.<sup>8,28</sup> Halide salts typically display higher melting points as compared to their NTf<sub>2</sub><sup>–</sup> analogues. The reduction in melting point upon greater degrees of fluorination may be attributed to the lower crystal lattice energy of the substances. The perfluoroalkyl groups exhibit very weak intermolecular forces, leading to lower melting points. To our surprise, both [4]Cl and [4]NTf<sub>2</sub> exhibited much higher melting points suggesting the branched C<sub>4</sub>F<sub>9</sub> structure had little effect in reducing the crystal lattice energies. An exotherm was observed after the glass transition, but before the melting point in the DSC trace for [4]NTf<sub>2</sub> at approximately 50 °C. Decomposition temperatures of compounds [1]Cl, [2]Cl, and [3]Cl were approximately 295 °C, while compounds [1]NTf<sub>2</sub>, [2]NTf<sub>2</sub>, and [3]NTf<sub>2</sub> were stable until approximately 370 °C. The decreased basicity of bis(trifluoromethylsulfonyl)imide relative to chloride likely inhibited the E2 decomposition pathway of the  $\beta$ -hydrogen by which phosphonium salts typically undergo when heated. The decomposition point of [4]Cl was found to be exceptionally low in comparison to its analogues. This led us to believe that an alternative decomposition pathway was present. We postulated that the electronegativity of the perfluoro-*tert*-butoxy group might allow for its displacement in the presence of a nucleophile (such as Cl<sup>–</sup>) at high temperatures. Deprotonation of a  $\beta$ -hydrogen to form perfluoro-*t*-butanol would result in decomposition (Scheme 2).

The plausibility of this mechanism is supported by the relative basicity between chloride and perfluoro-*tert*-butoxide, with their conjugate acids having pK<sub>a</sub> values of –7 and 5.2, respectively. The increase in thermal stability from 198 to 389 °C upon ion exchange with the bulky, non-nucleophilic NTf<sub>2</sub><sup>–</sup> anion also supports this mechanism. We decided to further investigate this phenomenon. Compound [4]Cl was heated slowly within a mass spectrometer and the fragments consistent with perfluoro-*tert*-butanol elimination were monitored. After 532 s, a positively charged fragment at  $m/z = 197$  was observed and attributed to [(CF<sub>3</sub>)<sub>3</sub>COH – (HF<sub>2</sub>)]<sup>+</sup>. Upon further heating, the signal at  $m/z = 197$  was observed at a maximum after 889 s. The experiment was repeated under identical conditions using [4]NTf<sub>2</sub> and no signal at  $m/z = 197$  was observed until 925 s, indicating greater thermal stability. Additionally, there was no evidence for the displacement or cleavage of the styrenic moiety from

**SCHEME 2** Decomposition pathway of [4]Cl under inert atmosphere.

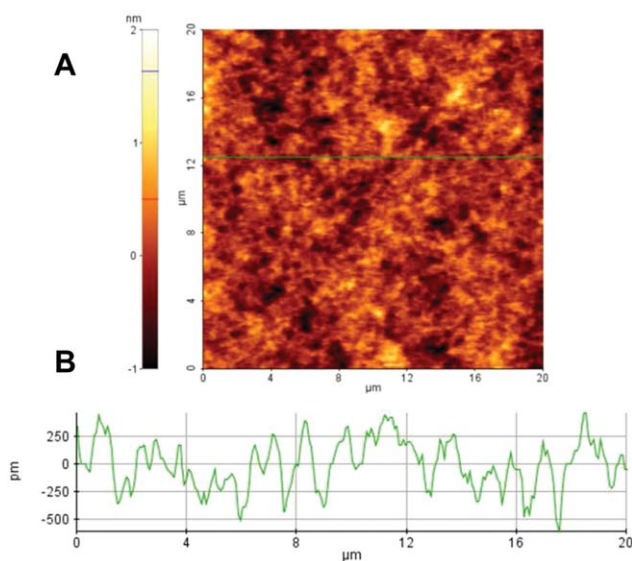


**FIGURE 3** (A) AFM image obtained in an area of  $20 \times 20 \mu\text{m}^2$  on a photopolymerized film containing 0.1 wt % [4]NTf<sub>2</sub> in HDDA (B) a profile isolated from the image as indicated in the insert line in (A).

the phosphonium salt. The slight increase in thermal stability of [4]NTf<sub>2</sub> relative to the other NTf<sub>2</sub> salts may be due to the reduced acidity of the  $\beta$ -hydrogen, as the electron-withdrawing fluorocarbon groups are further in distance. This is supported by the chemical shifts in the <sup>1</sup>H NMR spectra ( $\delta = 2.1$  for [4]NTf<sub>2</sub> and  $\sim 3.1$  for [1–3] NTf<sub>2</sub>).

### Hydrophobic Surface Modification using HFPPS

Compounds [1]–[4]Cl were initially screened for their potential use as a fluorinated additive to UV-curable resins (HDDA). Low surface energy materials (such as fluorocarbons) are known to migrate to the liquid–air interface prior to photopolymerization.<sup>19,20</sup> Initial attempts at solventless polymerization were problematic because of their insolubility in HDDA. Attempts to dissolve the mixture with acetone resulted in the formation of emulsions, translating to hazy films after polymerization. Additional acetone (60–70% by mass) did not remove the emulsion suggesting that changes to the molecular structure of our salts were crucial to increase compatibility. It is well established that the solubility of phosphonium salts is highly dependent on both the anion and cation composition, thus, we decided to utilize the hydrophobic bis(trifluoromethylsulfonyl)imide anion in conjunction with our fluorinated phosphonium cation.

Compounds [1]–[4]NTf<sub>2</sub> displayed excellent solubility in HDDA with mild heating and stirring. Upon irradiation, the free flowing solution hardened into a transparent, colorless film within seconds. AFM analysis of films containing 0.1 wt % of compounds [1]–[4]NTf<sub>2</sub> in HDDA was conducted to determine surface roughness, as micro/nano-features are known to change the hydrophobicity of surfaces. We found that the surfaces were essentially flat with a root-mean square roughness of 0.2–0.3 nm over a  $20 \times 20 \mu\text{m}^2$  scan

window (Supporting Information Fig. S-32). A line profile of a representative sample can be seen in Figure 3. There are no detectable surface features that could contribute to the wetting properties of these polymers.

We then evaluated the static water contact angles of films containing various amounts of compounds [1]–[4]NTf<sub>2</sub>. Upon increasing the concentration of compound [1]NTf<sub>2</sub> in HDDA from 0.1 to 1.5 wt %, the WCA increased from 55° on pristine HDDA films to 87° with 1.5 wt % loading (Table 2).

A WCA increase of 32° with low fluorinated HFPPS loading is indicative of fluorine migration to the surface. To impart greater degrees of hydrophobicity, we replaced the isooctyl group with an additional perfluorobutyl chain. Upon the addition of [2]NTf<sub>2</sub> to HDDA from 0.05 to 1 wt %, the WCA increased from 55° to 92° (Table 2). Despite both [1]NTf<sub>2</sub> and [2]NTf<sub>2</sub> having similar performances at higher loadings, the onset for increasing WCA was shifted significantly with less material required to attain similar contact angles for [2]NTf<sub>2</sub>. These results are significant as they reveal that the replacement of the isooctyl group with a perfluorobutyl chain did not greatly alter the peak hydrophobic effect, but rather shifted the onset where it occurred. By comparing the 1 wt% loading of [1]NTf<sub>2</sub> and the 0.1 wt % loading of [2]NTf<sub>2</sub>, it is clear that they have similar contact angles, yet possess vastly different fluorine economies. Formulations possessing [1]NTf<sub>2</sub> require eight times as many fluorine atoms as [2]NTf<sub>2</sub> to obtain similar hydrophobic effects. Passivation of polymer surfaces with fluorocarbons depends not only on fluorine content, but also molecular architecture imparting fluorocarbon behavior. Very small amounts of fluorinated salts, despite bearing charges, have the capability to decrease the wettability of photopolymerized surfaces. The capacity to tune the properties of such systems using salts as opposed to standard fluorocarbons may offer new prospects where both charged species and hydrophobicity are desired within a photopolymerizable system.

Despite such findings, the hydrophobic performance of [1]NTf<sub>2</sub> and [2]NTf<sub>2</sub> were noticeably lower than other fluorinated materials on smooth surfaces such as Teflon (WCA = 115°), or compared to other hydrophobic UV-cured systems.<sup>19</sup> This is likely the result of reduced crystallization of the perfluorobutyl groups at the interface. It is well

**TABLE 2** WCA for all HFPPS as a Function of wt % in HDDA

wt %	[1]NTf <sub>2</sub>	[2]NTf <sub>2</sub>	[3]NTf <sub>2</sub>	[4]NTf <sub>2</sub>
0	55 ± 3	55 ± 3	55 ± 3	55 ± 3
0.01	–	–	91 ± 1	73 ± 1
0.05	–	80 ± 1	97 ± 2	90 ± 1
0.1	82 ± 1	89 ± 1	98 ± 1	94 ± 1
0.5	84 ± 1	91 ± 1	101 ± 2	97 ± 2
1	87 ± 1	92 ± 1	–	95 ± 1
1.5	84 ± 1	92 ± 1	–	93 ± 2

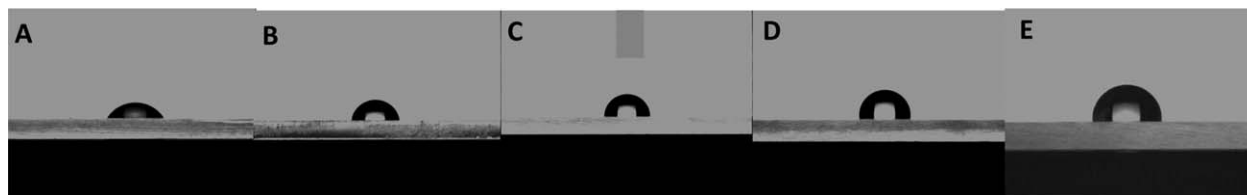


**FIGURE 4** WCAs of droplets on A) HDDA B) 1.5 wt % of [1]NTf<sub>2</sub> C) 1.5 wt % of [2]NTf<sub>2</sub> D) 1 wt % of [3]NTf<sub>2</sub> and E) 0.5 wt % of [4]NTf<sub>2</sub>.

established that longer fluorocarbon chains are capable of undergoing side-chain crystallization at the surface, resulting in much higher degrees of hydrophobicity.<sup>26</sup> Reduced ordering of the perfluoroalkyl chains allows water to permeate around the fluorocarbon groups, thus lowering the WCA. For greater performance, we decided to test the efficacy of perfluorinated octyl chains on our phosphonium ion scaffold as a model system. The WCA increased from 55° for pristine HDDA, to 91° with only a 0.01 wt % loading of [3]NTf<sub>2</sub>. Further addition slowly raised the WCA to 101° at 1 wt % (Table 2). Attempts to add additional compound unfortunately resulted in phase separation and poor quality films. In comparison to [1]NTf<sub>2</sub> and [2]NTf<sub>2</sub>, higher degrees of hydrophobicity with a steeper onset was observed when using [3]NTf<sub>2</sub>. These results indicate that phosphonium salts with longer fluorocarbon chains provide enhanced anti-wetting properties of photopolymerized films, consistent with our previous hydrophobic phosphonium studies.<sup>28</sup> Despite the excellent performance of perfluorooctyl-derived materials within the literature, their bioaccumulation properties renders them a consistent threat to wildlife and humans alike. In light of this reality, we were inspired to investigate the properties of branched perfluoroalkyl groups for hydrophobic applications. We believed that the superb hydrophobicity and steric encumbrance of a phosphonium salt bearing nine —CF<sub>3</sub> groups would passivate the surface and exhibit similar performance to the perfluorooctyl moieties. Upon addition of 0.01–1.5 wt % of [4]NTf<sub>2</sub> to HDDA, we observed a pronounced increase in the WCA, surpassing that of [1]NTf<sub>2</sub> and [2]NTf<sub>2</sub>, and with similar performance to [3]NTf<sub>2</sub> (WCA = 97°). Increased solubility of [4]NTf<sub>2</sub> compared to [3]NTf<sub>2</sub> was also observed allowing for loadings >1 wt %, however with reduced WCA. Using this new molecular structure, we negate the bioaccumulation issues associated with perfluorooctyl groups while simultaneously boosting our fluorine economy, as we provided very similar WCAs using 27 fluorine atoms per cation ([4]<sup>+</sup>) as opposed to 34 ([3]<sup>+</sup>). Figure 4 illustrates the hydrophobic effect as the phosphonium salt is varied.

To determine the mechanism of increased hydrophobicity, the exact nature of the interface was investigated to gain insight into whether or not the fluorinated salt migrates to the surface. To test this hypothesis, TOF-SIMS was employed to examine the composition of the surface material. This technique was chosen due to its surface sensitivity and its capability to identify molecular fragments and to analyze surfaces on the nanometer depth scale.<sup>29,30</sup>

A photopolymerized film containing 1 wt % of [1]NTf<sub>2</sub> was analyzed using the procedure discussed in the experimental section. A negative ion mass spectrum was obtained and an abundant peak at mass/charge ratio (*m/z*) 280 was assigned to C<sub>2</sub>F<sub>6</sub>S<sub>2</sub>O<sub>4</sub>N<sup>−</sup>, which is the anion [NTf<sub>2</sub>]<sup>−</sup>. It is clear from the ion mass spectrum that there are various fragments of the anion, such as CF<sub>3</sub>S<sub>2</sub>O<sub>3</sub>N<sup>−</sup>, CF<sub>3</sub>SO<sub>2</sub>N<sup>−</sup>, CF<sub>3</sub>SO<sub>2</sub><sup>−</sup>, SO<sub>2</sub>N<sup>−</sup>, and SON<sup>−</sup> (Fig. 5). Other abundant peaks are O<sup>−</sup>, F<sup>−</sup>, hydrocarbons (e.g., C<sub>2</sub>H<sup>−</sup> and C<sub>4</sub>H<sup>−</sup>), CN<sup>−</sup>, and C<sub>x</sub>H<sub>y</sub>O<sub>z</sub><sup>−</sup>. The cation of the photopolymerized film containing 1 wt % of [1]NTf<sub>2</sub> is detected in the positive ion mass spectrum (not shown).

As shown in Figure 6, depth profiles of negative ion fragments of interest (O<sup>−</sup>, CF<sup>−</sup>, C<sub>2</sub>H<sup>−</sup>, and [NTf<sub>2</sub>]<sup>−</sup>) were obtained as the surface of the sample containing 1 wt % [1]NTf<sub>2</sub> was ablated with a 3 keV Cs<sup>+</sup> sputter beam. The depth was obtained with a sputter rate of 0.08 nm/s, which was estimated by sputtering a PET film and measuring the crater depth. Upon continued ablation up to 3 nm, the ion intensity for the anion [NTf<sub>2</sub>]<sup>−</sup> dropped dramatically. The CF<sup>−</sup> ion fragment was also detected at high intensity in the first bombardments, and its intensity dropped off significantly, with a similar time frame for the [NTf<sub>2</sub>]<sup>−</sup> anions. These severe reductions in ion detection not only confirm that the [NTf<sub>2</sub>]<sup>−</sup> containing HFPPS was more concentrated at

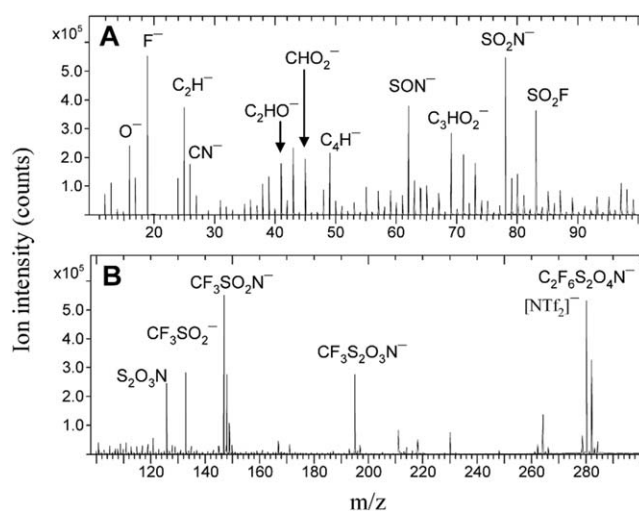


**FIGURE 5** Negative ion mass spectrum in *m/z* ranges of 10–100 (A) and 100–300 (B) obtained on the surface of a photopolymerized film containing 1 wt % of [1]NTf<sub>2</sub> in HDDA.

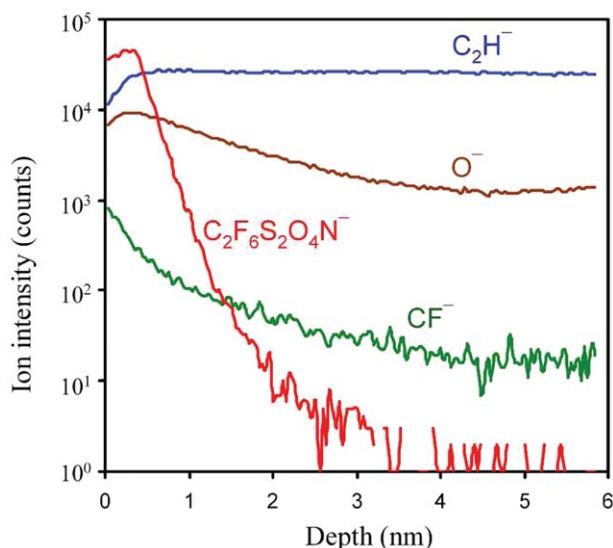


**FIGURE 6** Depth profiles of negative ion fragments of  $O^-$ ,  $CF^-$ ,  $C_2H^-$ , and  $C_2F_6S_2O_4N^-$  (which is the anion  $[NTf_2]^-$ ) obtained using a 3 keV  $Cs^+$  beam to sputter the surface and a 25 keV  $Bi_3^+$  ion beam to analyze the surface.

the top of the film but also that there was minimal  $CF^-$  left beneath the surface.

Our TOF-SIMS results thus suggest that the phosphonium salt accumulated at the air–polymer interface of the photopolymerized film. The depth profile of  $[NTf_2]^-$  shown in Figure 6 indicates that the ions accumulated mainly within 3 nm of the surface, likely a direct result of the fluorinated phosphonium salt.

In contrast, ion fragments associated with both the polyacrylate and HFPPS ablated under the same conditions (i.e.,  $O^-$  and  $C_2H^-$ ) remained relatively constant throughout the experiment. The tendency of the anionic sections of the HFPPS to remain unfragmented and charged under experimental conditions is ideal, and has proven to be an excellent handle for TOF-SIMS analysis. We believe that this technique may be applied to other ammonium/phosphonium salts in materials applications.

## CONCLUSIONS

An array of HFPPS were synthesized and characterized for their physical and chemical properties. Exchanging the chloride for bis(trifluoromethylsulfonyl)imide resulted in improved solubility in HDDA and increased thermal stability for all phosphonium cations. Through the alteration of the phosphonium salt, either with increased fluorine loading, or through architecture manipulation, a structure–activity relationship was observed. Greater degrees of fluorination increased both the maximum attainable contact angle, along with its onset.  $[4]NTf_2$  imbued films with water repellent properties with similar efficacy to its perfluorooctyl analogue without the bioaccumulation issues. TOF-SIMS confirmed the presence of HFPPS at the surface, and demonstrated for the

first time that charged species could be selectively directed to a desired location in photopolymerizable systems. The fluorocarbon appendages acted as a shuttle for the charged molecules, forcing the ions to the polymer/air interface. Future work will include the attachment of an additional functionality to the fluorinated phosphorus centre in an attempt to modify the surface with a desired moiety. There are also prospects to access the surface charge through an ion-exchange process with the photopolymer allowing for surface modification of UV-cured films with very low HFPPS loading.

## ACKNOWLEDGMENTS

The authors thank Cytec Industries, the Natural Sciences and Engineering Research Council through its Discovery Grant and Strategic Project Grant programs (NSERC-DG; NSERC-SPG), Ontario Ministry of Research and Innovation (OMRI), and Western University Canada for generous support. The Chemistry Workshop J. Vanstone and J. Aukema are thanked for construction of the  $PH_3$  line and necessary accessories.

## REFERENCES AND NOTES

- 1 C. Hiemstra, W. Zhou, Z. Y. Zhong, M. Wouters, J. Feijen, *J. Am. Chem. Soc.* **2007**, *129*, 9918–9926.
- 2 T. A. Schaedler, A. J. Jacobsen, A. Torrents, A. E. Sorensen, J. Lian, J. R. Greer, L. Valdevit, W. B. Carter, *Science* **2011**, *334*, 962–965.
- 3 S. Gu, R. Cai, T. Luo, K. Jensen, C. Contreras, Y. S. Yan, *ChemSusChem* **2010**, *3*, 555–558.
- 4 E. R. Kenawy, F. I. Abdel-Hay, A. Abou El-Magd, Y. Mahmoud, *React. Funct. Polym.* **2006**, *66*, 419–429.
- 5 E. R. Kenawy, Y. A. G. Mahmoud, *Macromol. Biosci.* **2003**, *3*, 107–116.
- 6 A. Popa, C. M. Davidescu, R. Trif, G. Iliu, S. Iliescu, G. Dehelean, *React. Funct. Polym.* **2003**, *55*, 151–158.
- 7 E. R. Kenawy, F. I. Abdel-Hay, A. El-Shanshoury, M. H. El-Newehy, *J. Polym. Sci. Part A: Polym. Chem.* **2002**, *40*, 2384–2393.
- 8 J. J. Tindale, C. Na, M. C. Jennings, P. J. Ragogna, *Can. J. Chem.* **2007**, *85*, 660–667.
- 9 B. M. Berven, R. O. Oviasuyi, R. J. Klassen, M. Idacavage, E. R. Gillies, P. J. Ragogna, *J. Polym. Sci. Part A: Polym. Chem.* **2012**, *51*, 499–508.
- 10 E. S. Hatakeyama, H. Ju, C. J. Gabriel, J. L. Lohr, J. E. Bara, R. D. Noble, B. D. Freeman, D. L. Gin, *J. Membr. Sci.* **2009**, *330*, 104–116.
- 11 S. Cheng, F. L. Beyer, B. D. Mather, R. B. Moore, T. E. Long, *Macromolecules* **2011**, *44*, 6509–6517.
- 12 S. Cheng, M. Zhang, T. Wu, S. T. Hemp, B. D. Mather, R. B. Moore, T. E. Long, *J. Polym. Sci. Part A: Polym. Chem.* **2012**, *50*, 166–173.
- 13 S. T. Hemp, M. H. Allen, Jr.; M. D. Green, T. E. Long, *Biomacromolecules* **2012**, *13*, 231–238.
- 14 N. S. Choi, J. K. Park, *Solid State Ionics* **2009**, *180*, 1204–1208.
- 15 D. Chen, Y. L. Zang, S. P. Su, *J. Appl. Polym. Sci.* **2010**, *116*, 1278–1283.
- 16 S. K. Kim, C. A. Guymon, *J. Polym. Sci. Part A: Polym. Chem.* **2011**, *49*, 465–475.

- 17** S. K. Kim, C. A. Guymon, *Polymer* **2012**, *53*, 1640–1650.
- 18** J. J. Tindale, P. J. Ragogna, *Chem. Commun.* **2009**, 1831–1833.
- 19** H. Miao, L. L. Cheng, W. F. Shi, *Prog. Org. Coat.* **2009**, *65*, 71–76.
- 20** M. Sangermano, R. Bongiovanni, M. Longhin, G. Rizza, C. M. Kausch, Y. Kim, R. R. Thomas, *Macromol. Mater. Eng.* **2009**, *294*, 525–531.
- 21** Z. Hu, L. M. Pitet, M. A. Hillmyer, J. M. DeSimone, *Macromolecules* **2010**, *43*, 10397–10405.
- 22** L. J. Alvey, D. Rutherford, J. J. J. Juliette, J. A. Gladysz, *J. Org. Chem.* **1998**, *63*, 6302–6308.
- 23** D. Szabo, J. Mohl, A. M. Balint, A. Bodor, J. Rabai, *J. Fluorine Chem.* **2006**, *127*, 1496–1504.
- 24** A. R. Stiles, F. F. Rust, W. E. Vaughan, *J. Am. Chem. Soc.* **1952**, *74*, 3282–3284.
- 25** US-EPA 2010/2015 PFOA Stewardship Program—<http://www.epa.gov/oppt/pfoa/pubs/stewardship/index.html> (accessed March 6), **2013**.
- 26** K. Honda, M. Morita, H. Otsuka, A. Takahara, *Macromolecules* **2005**, *38*, 5699–5705.
- 27** E. F. Hare, E. G. Shafrin, W. A. Zisman, *J. Phys. Chem.* **1954**, *58*, 236–239.
- 28** C. Emnet, K. M. Weber, J. A. Vidal, C. S. Consorti, A. M. Stuart, J. A. Gladysz, *Adv. Synth. Catal.* **2006**, *348*, 1625–1634.
- 29** A. Benninghoven, *Angew. Chem. Int. Ed. Engl.* **1994**, *33*, 1023–1043.
- 30** M. S. Wagner, *Anal. Chem.* **2005**, *77*, 911–922.